collection. A linear decay correction was made to account for this change. In reducing the data, Lorentz and polarization factors were applied, as well as an empircial absorption correction based on the measurement of five reflections having ψ values near 90°.[45] The structure was solved by MULTAN,[44] which revealed the positions of the two Br atoms in the asymmetric unit. The latter was comprised of $^1/_3$ CBr_4 and $^1/_3$ quinuclidine, both lying on three-fold axes and thus forming a 1:1 complex. The remaining non-hydrogen atoms were located in subsequent difference Fourier syntheses; however the least-squares refinement was found to be quite insensitive to the positional or thermal parameters of the non-bromine atoms. They were accordingly refined isotropically. The CBr_4 appears to be significantly different from ideal sp^3 geometry due probably to poor positioning of C_1. An attempt to idealize it by holding C_1 fixed at 0.101, 0.101, 101 resulted in essentially no change in the R value. Thus the true geometry of this acceptor molecule is unsure. The hydrogen atoms were entered in ideal locations, with isotropic temperature factors estimated on the basis of the thermal motion of the associated carbons. After all shift/esd ratios were less than 0.2, convergence was reached at the agreement factors listed in Table III. No unusually high correlations were noted between any of the variables in the last cycle of least-squares refinement, and the final difference density map showed no peaks greater than 0.90 e Å^{-3}. The correct absolute configuration was determined by refining the inverse structure to $R = 0.052$, indicating the reported atomic coordinates to be correct. All calculations were made by using Molecular Structure Corporation's TEXRAY 230 modifications of the SDP-PLUS series of programs. The final fractional positional parameters for the quinuclidine–CBr_4 complex are included in Table VIII.

The donor and acceptor components of the EDA complex of quinuclidine and CBr_4 are well-defined in the crystal. The ORTEP diagram in Figure 8 shows one of the discrete donor–acceptor pairs in isolation. The relevant N···Br distance of 2.53 Å is about an angstrom less than the sum of the van der Waals radii of 3.5.[37] Furthermore it is significantly shorter than the corresponding nonbonded contacts of 2.88 and 2.76 Å in the Dabco–CBr_4 complex. The difference between quinuclidine and Dabco may reside in the extra ground-state stabilization of the latter as a result of the transannular interaction of the two nitrogens[46] and indicated by its weaker base strength.[47] The linear C–Br···N arrangement emphasizes the optimum CT interaction of the n-HOMO centered on nitrogen with the σ^* LUMO of the Br–C bond. Thus the CT chromophoric unit in the EDA complex of quinuclidine and CBr_4 consists essentially of the same close nonbonded interaction between nitrogen and bromine as it is in the Dabco–CBr_4 complex (vide supra). Otherwise the comparison of the solid-state CT spectra in Figure 7 merely reflects quantitative differences in these amine donors. The quinuclidine moiety is well-resolved in the crystal of the EDA complex in contrast to the extensive disorder in the crystal of quinuclidine itself.[49] However, there is some ambiguity of the carbon location in the acceptor (vide supra), unlike that in the crystal of CBr_4 itself.[50]

Acknowledgment. We thank J. D. Korp for assistance with the crystal structure, J. S. Frye of the Colorado State University Regional NMR Center (funded by National Science Foundation Grant no. CHE-8208821), and the National Science Foundation and Robert A. Welch Foundation for financial support.

Supplementary Material Available: Tables of the observed and calculated structure factors for the Dabco–CBr_4 and quinuclidine–CBr_4 complexes (5 pages). Ordering information is given on any current masthead page.

---

(45) North, A. C. T.; Phillips, D. D.; Matthews, F. S. *Acta Crystallogr., Sect. A* **1968** *24*, 351.

(46) Compare: Hoffmann, R. *Acc. Chem. Res.* **1971**, *4*, 1.

(47) The pK_b values of Dabco and quinuclidine are 5.3 and 3.4, respectively.[48]

(48) (a) Wepster, B. M. *Recl. Trav. Chim. Pays-Bas* **1952**, *71*, 1171. (b) *Merck Index*, Xth Ed., Rahway, NJ, 1983.

(49) Fourme, R. *J. Phys. (Paris)* **1979**, *40*, 557.

(50) More, M.; Baert, F.; Lefebvre, J. *Acta Crystallogr., Sect. B.* **1977**, *33*, 3681.

Permanganate Ion Oxidations. 18. Kinetics and Mechanism of the Oxidation of (*E*)-3-(2-Pyridinyl)-, (*E*)-3-(3-Pyridinyl)-, and (*E*)-3-(4-Pyridinyl)-2-propenoates[1]

Fillmore Freeman,* Lilian Y. Chang,[2a] John C. Kappos,[2b] and Linga Sumarta

Department of Chemistry, University of California, Irvine, Irvine, California 92717

Received August 11, 1986

The kinetics and mechanism of the permanganate ion oxidation of (*E*)-3-(2-pyridinyl)-, (*E*)-3-(3-pyridinyl)-, (*E*)-3-(4-pyridinyl)-, (*E*)-6-methyl-3-(2-pyridinyl)-, (*E*)-2-methyl-3-(3-pyridinyl)-, and (*E*)-2-cyano-3-(3-pyridinyl)-2-propenoate have been studied at 418 nm and 526 nm in phosphate-buffered solutions (pH 6.83 ± 0.03). The rate law $\nu = k[MnO_4^-][\text{substrate}]$ was observed. The structure of the activated complex, the influence of substituents on the rate of oxidation, the philicity of permanganate ion, and the possible autocatalytic role of soluble (colloidal) manganese dioxide are discussed.

Although the permanganate ion oxidation of alkyl-substituted and phenyl-substituted alkenes has received considerable study,[3-12] there is only one report that involves heterocycle-substituted olefins.[1] None of these studies has presented direct or unambiguous evidence for existence of the long-sought elusive four-membered metallacyclooxetane (1; [2 + 2] cycloaddition) or cyclic manganate(V)

---

(1) Part 17: Freeman, F.; Chang, L. Y. *J. Am. Chem. Soc.* **1986**, *108*, 4504.

(2) (a) University of California, Irvine, President's Undergraduate Fellow, 1985–86; University of California, Irvine, Undergraduate Research Fellow, 1985–86. (b) University of California, Irvine, President's Undergraduate Fellow, 1984–86; University of California, Irvine, Undergraduate Research Fellow, 1985–86.

(3) Freeman, F.; Kappos, J. C. *J. Org. Chem.* **1986**, *50*, 1654.

(4) Freeman, F. *React. Species Chem. React.* **1976**, *1*, 179.

(5) Wiberg, K. B.; Geer, R. D. *J. Am. Chem. Soc.* **1966**, *88*, 5827.

(6) Simândi, L. I.; Jâky, M. *J. Am. Chem. Soc.* **1976**, *98*, 1995.

(7) (a) Lee, D. G.; Brownridge, J. R. *J. Am. Chem. Soc.* **1973**, *95*, 3033. (b) Lee, D. G.; Brownridge, J. R. *J. Am. Chem. Soc.* **1974**, *96*, 5517.

(8) Lee, D. G.; Nagarajn, K. *Can. J. Chem.* **1984**, *63*, 1018.

(9) Freeman, F.; Kappos, J. C. *J. Am. Chem. Soc.* **1985**, *107*, 6628.

(10) Freeman, F.; Fuselier, C. O.; Armstead, C. R.; Dalton, C. E.; Davidson, P. A.; Karchefski, E. M.; Krochman, D. E.; Johnson, M. N.; Jones, N. K. *J. Am. Chem. Soc.* **1981**, *103*, 1154.

(11) Freeman, F.; Fuselier, C. O.; Karchefski, E. M. *Tetrahedron Lett.* **1975**, 2133.

(12) Simândi, L. I.; Jâky, M.; Freeman, F.; Fuselier, C. O.; Karchefski, E. M. *Inorg. Chim. Acta* **1978**, *31*, L457.

diester intermediate (**2**; [4 + 2] cycloaddition).[13-15]

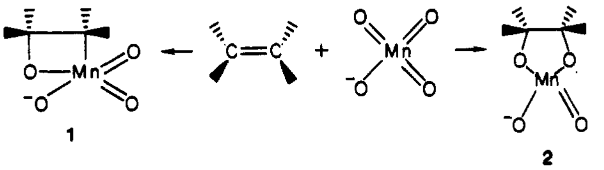

(1)

1 **2**

Since it is known that acid chromate ion ($HCrO_4^-$) is stabilized by 2-pyridinecarboxylic acid (**3**)[16a,b] and that cyclic osmate esters are stabilized by pyridine (**4**),[16c] we have investigated the permanganate ion oxidation of (*E*)-3-(2-pyridinyl)- (**5**), (*E*)-3-(3-pyridinyl)- (**6**), (*E*)-3-(4-pyridinyl)- (**7**), (*E*)-6-methyl-3-(2-pyridinyl)- (**8**), (*E*)-2-methyl-3-(3-pyridinyl)- (**9**), and (*E*)-2-cyano-3-(3-pyridinyl)-2-propenoate (**10**) in order to determine whether ligand coupling between reductant or excess reductant and the reduced form of the oxidant would occur to give stable complexes or cyclic intermediates similar to **1** and **2**. In addition, kinetic data were needed in order to compare the rate of permanganate ion oxidation of pyridinyl-substituted alkenes with thienyl-substituted and phenyl-substituted olefins. Data that relate to the above questions are presented in this report.

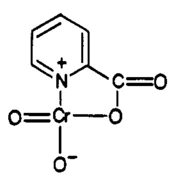

3

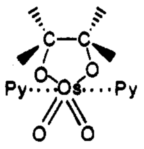

4

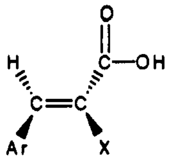

	Ar	X
5	2-pyridinyl	H
6	3-pyridinyl	H
7	4-pyridinyl	H
8	6-methyl-2-pyridinyl	H
9	3-pyridinyl	CH_3
10	3-pyridiny	CN

Experimental Section

Melting points were determined in open capillary tubes with a Thomas-Hoover apparatus and are uncorrected. Elemental analyses were performed by Robertson Laboratory, Inc., Florham Park, NJ.

IR spectra were obtained with a Perkin-Elmer 283 spectrophotometer, calibrated with the 1601-cm^{-1} absorption of polystyrene, in CCl_4, as neat films, or as KBr disks.

High resolution mass spectra were obtained with a VG 7070E-HF mass spectrometer (70 eV). Medium resolution mass spectra were obtained with a Finnigan 9610 GC-EI-CI mass spectrometer with a Nova 3 data system operating at an ionization potential of 70 or 100 eV. Chemical ionization (CI) mass spectra were obtained by using 2-methylpropane as the reactant gas.

^1H NMR spectra were recorded at 80 MHz (Varian FT-80A), at 250 MHz (Bruker WM-250), and at 300 MHz (GE/Nicolet 300) with the solvent(s) noted. Chemical shifts (δ) are reported downfield from internal Me_4Si (0.5% for Fourier transform) at $\delta = 0.00$ ppm. Apparent coupling constants (J) are reported in hertz (Hz). Because of the data digitization with the FT instrument, J values are ±0.40 Hz maximum, but normally are accurate to ±0.20 Hz. ^{13}C NMR data were obtained with a Bruker WM-250 spectrometer and a GE/Nicolet 300-MHz spectrometer.

Solutions were prepared immediately before use in water that had been deionized and then slowly distilled from an all-glass Corning mega-pure apparatus. Appropriate quantities of KH_2PO_4 and Na_2HPO_4 to maintain pH and ionic strength were dissolved in the substrate solution. Ionic strength was also adjusted by adding KCl to the permanganate solution when necessary. Standard (Titrisol) potassium permanganate solutions were used. The pH values were determined on an Altex 60 pH meter in the buffered substrate solution before reaction and in the product mixture after oxidation.

The kinetics were determined on a Durrum Model D-110 stopped-flow spectrometer that was connected to a Tracor-Northern 1710 multichannel analyzer. The data were transferred to an IBM PC for analysis and printing. Temperature was maintained with a Forma Model 2095-2 refrigerated and heated bath circulator.

Kinetic experiments were performed under pseudo-first-order conditions with a large excess of substrate. The rates were determined by monitoring the disappearance of permanganate ion at 526 nm and by observing the rate of formation of soluble (colloidal) manganese dioxide at 418 nm. The pseudo-first-order rate constants (k_ψ) were calculated from plots of $-\ln (A_t - A_\infty)$ vs. time at 526 nm or $-\ln (A_\infty - A_t)$ vs. time at 418 nm on a first-order kinetics program. All rate constants are the average of two or more experiments.

The ultraviolet-visible spectra of manganese dioxide were obtained on a Cary 219 spectrophotometer.

(*E*)-3-(2-Pyridinyl)-2-propenoic acid (**5**, mp 202–203 °C [lit.[17] mp 202–203 °C]) and **(*E*)-3-(4-pyridinyl)-2-propenoic acid** (**7**, mp 290–292 °C [lit.[18] mp 296–297 °C]) were prepared from the corresponding aldehyde and propanedioic acid. **(*E*)-3-(3-Pyridinyl)-2-propenoic acid** (**6**, mp 232–234 °C [lit.[19] mp 232–235 °C]) is commercially available.[20] Spectral data for **5**–**7** agreed with literature values.[21]

(*E*)-3-(6-Methyl-2-pyridinyl)-2-propenoic acid (**8**, mp 168.5–170 °C [lit.[22] mp 166–168 °C]) was prepared from 6-methyl-2-pyridinecarboxaldehyde and propanedioic acid.[22]

(*E*)-2-Methyl-3-(3-pyridinyl)-2-propenoic acid (**9**) was prepared by condensation of 3-pyridinecarboxaldehyde and propanedioic acid (21 h reflux, 53% yield):[1,23] mp 189–191 °C; EIMS, m/z calcd for $C_9H_9NO_2$ 163.0633; obsd 163.0641.

(*E*)-2-Cyano-3-(3-pyridinyl)-2-propenoic acid (**10**) was prepared from 3-pyridinecarboxaldehyde and 2-cyanoethanoic acid:[1,24] mp 210–212 °C; EIMS, m/z calcd for $C_9H_6N_2O_2$ 174.0429; obsd 174.0428.

Results and Discussion

The rate of disappearance of permanganate ion during the oxidation of (*E*)-3-(3-pyridinyl)-2-propenoate (**6**) was determined at 526 nm and the rate of formation of soluble (colloidal) manganese dioxide was monitored at 418 nm.

---

[13] Sharpless, K. B.; Teraniski, A. Y.; Bäckvall, J. E. *J. Am. Chem. Soc.* **1977**, *99*, 3120.

[14] (a) Rappé, A. K.; Goddard, W. A., III. *J. Am. Chem. Soc.* **1982**, *104*, 448. (b) Rappé, A. K.; Goddard, W. A., III. *J. Am. Chem. Soc.* **1982**, *104*, 3287.

[15] Walba, D. M.; Wand, M. D.; Wilkes, M. C. *J. Am. Chem. Soc.* **1979**, *101*, 4396.

[16] (a) Peng, T.-Y.; Roček, J. *J. Am. Chem. Soc.* **1976**, *98*, 1026. (b) Roček, J.; Peng, T.-Y. *J. Am. Chem. Soc.* **1977**, *99*, 7622. (c) Criegee, N. R.; Marchand, B.; Wannowius, H. *Liebigs Ann. Chim.* **1941**, *550*, 99.

[17] Tullock, C. W.; McElvain, S. M. *J. Am. Chem. Soc.* **1939**, *61*, 961.

[18] (a) Katritzky, A. *J. Chem. Soc.* **1955**, 2581. (b) Stoicescu, C. *Rev. Roum. Chim.* **1983**, *28*, 147. (c) Kleiman, M.; Weinhouse, S. *J. Org. Chem.* **1945**, *10*, 562.

[19] Dornow, A.; Schacht, W. *Chem. Ber.* **1947**, *80*, 505.

[20] Aldrich Chemical Co.

[21] Zuccarello, F.; Buemi, G.; Fasone, S.; Gandolfo, C.; Raudino, A.; Grasso, D. *Z. Phys. Chem. (Wiesbaden)* **1982**, *130*, 63.

[22] Cahill, R.; Crabb, T. A. *Org. Magn. Reson.* **1973**, *5*, 505.

[23] Miller, R. E.; Nord, F. F. *J. Org. Chem.* **1949**, *15*, 89.

[24] Cope, A. C.; D'Addieco, A. A.; Whyte, D. E.; Glickman, S. A. *Organic Syntheses*; Wiley: New York, 1963; Collect. Vol. IV, p 234.

Table I. Kinetic Data from the Permanganate Ion Oxidation of (*E*)-3-(3-Pyridinyl)-2-propenoate (6)[a]

10^3[(*E*)-3-(3-pyridyl)-2-propenoate], M	10^4[MnO_4^-], M	[KH_2PO_4],[b] M	pH	μ[c]	*k*,[d] M^{-1} s^{-1} 418 nm	*k*,[d] M^{-1} s^{-1} 526 nm
1.99	4.00	0.20	6.82	0.80	777 ± 15	677 ± 6
4.00	4.00	0.20	6.81	0.80	724 ± 1	720 ± 3
6.00	4.00	0.20	6.81	0.80	761 ± 22	691 ± 5
8.00	4.00	0.20	6.81	0.80	768 ± 23	687 ± 4
4.00	2.00	0.20	6.83	0.80	730 ± 4	734 ± 7
4.00	6.00	0.20	6.84	0.80	794 ± 34	620 ± 14
4.00	4.00	0.10	6.82	0.40	619 ± 5	526
4.00	4.00	0.30	6.82	1.20	820 ± 9	783 ± 12
4.00	4.00	0.40	6.83	1.60	1117 ± 37	896 ± 39
4.00	4.00	0.025	6.31	0.80[e]	952 ± 13	720 ± 4
4.00	4.00	0.05	6.57	0.80[e]	889 ± 11	716 ± 5
4.00	4.00	0.10	6.68	0.80[e]	787 ± 10	730 ± 4

[a] Temperature = 25.0 °C. [b] [KH_2PO_4] = [Na_2HPO_4]. [c] Ionic strength. [d] Second-order rate constant = $k = k_\psi$/[anion]. [e] Ionic strength adjusted with KCl.

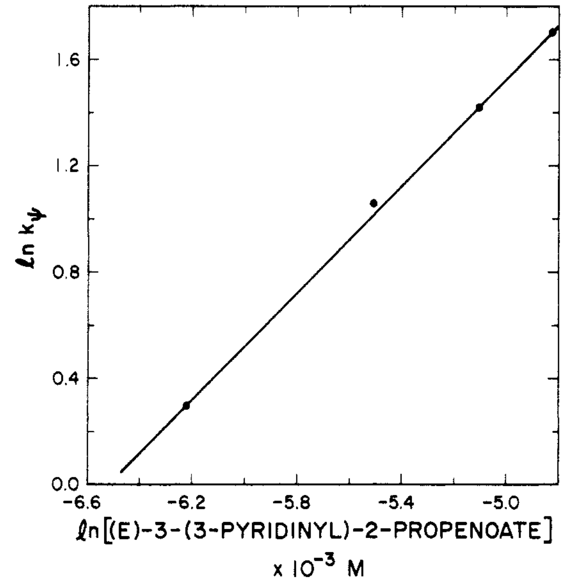

Figure 1. Plot of ln k_ψ vs. ln [(*E*)-3-(3-pyridinyl)-2-propenoate] at 525 nm in 0.20 M KH_2PO_4–Na_2HPO_4 (pH 6.82 ± 0.02, μ = 0.80) at 25.0 °C (slope = 1.00, correlation coefficient = 0.998).

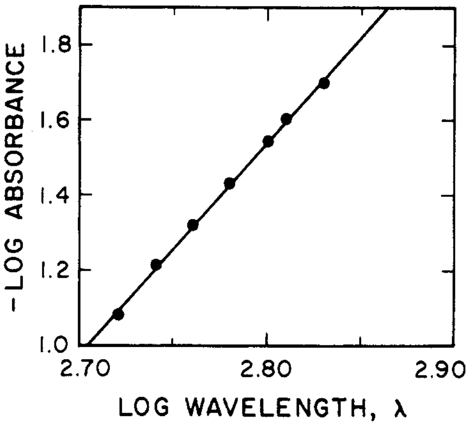

Figure 2. Rayleigh's law plot (–log absorbance vs. log wavelength) from the spectrum recorded after the reaction between (*E*)-3-(3-pyridinyl)-2-propenoate (6, 4 × 10^{-3} M) and permanganate ion (4 × 10^{-4} M). [KH_2PO_4] = [Na_2HPO_4] = 0.20 M, μ = 0.80, pH 6.81, temp = 25.0 °C; slope = 5.60, correlation coefficient = r = 0.999.

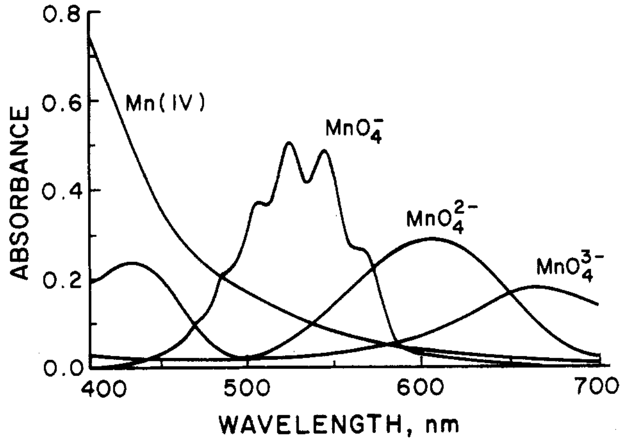

Figure 3. Ultraviolet–visible spectra of manganese species in the oxidation state IV–VII: 2 × 10^{-4} M solutions; 1-cm cells; temp = 20 °C. Reprinted with permission from *J. Am. Chem. Soc.* **1985**, *107*, 4220.[38a]

A first-order dependence on the concentration of permanganate ion is consistent with the linearity of pseudo-first-order plots (–ln (A_t –A $_\infty$) vs. time at 526 nm and –ln (A_∞ – A_t) vs. time at 418 nm) and the similar values of the pseudo-first-order rate constants (k_ψ) at 526 nm when the concentrations of buffers (KH_2PO_4–Na_2HPO_4) and (*E*)-3-(3-pyridinyl)-2-propenoate anion (**6**) were held constant and the concentration of permanganate ion was varied (Table I).

A first-order dependence on the concentration of (*E*)-3-(3-pyridinyl)-2-propenoate (**6**) is shown by the value of the second-order rate constant (Table I), the plot of k_ψ vs. [anion of **6**] that gives a straight line passing through the origin, and the plot of ln k_ψ vs. ln [anion of **6**] which is linear with a slope of unity (Figure 1).

The rate of oxidation increases with increasing ionic strength (Table I) as expected for a reaction between two negative ions. At constant ionic strength and varying buffer concentration, the rate of disappearance of permanganate ion at 526 nm does not change while the rate of formation of soluble (colloidal) manganese dioxide appears to increase with decreasing buffer concentration (Table I).[25] The colloidal particles of manganese dioxide formed in solution are stabilized by adsorption of phosphate ions ($H_2PO_4^-$, HPO_4^{2-}) on their surfaces.[1,3,9-12,26-32]

---

[25] The change in pH results from the KCl that was added in order to adjust ionic strength.

[26] Stewart, R. In *Oxidation in Organic Chemistry*, Part A; Wiberg, K. B., Ed.; Academic Press: New York, 1965, p 6.

[27] Wiberg, K. B.; Stewart, R. *J. Am. Chem. Soc.* **1955**, *77*, 1786.

[28] Freeman, F.; Karchefski, E. M. *Biochim. Biophys. Acta* **1976**, *447*, 238.

[29] (a) Narita, E.; Okabe, T. *Ind. Eng. Chem. Prod. Res. Dev.* **1982**, *21*, 662. (b) Narita, E.; Okabe, T. *Bull. Chem. Soc. Jpn.* **1980**, *53*, 525.

Table II. Effects of Aromatic Ring Systems on the Permanganate Ion Oxidation of (*E*)-2-Propenoates[a]

substrate	experimental conditions				
		pH	μ^b	k, $M^{-1}\ s^{-1}$	ref
(*E*)-3-phenyl-2-propenoic acid	0.99 M $HClO_4$, H_2O			1560[c]	5–7
(*E*)-3-phenyl-2-propenoic acid	1.01 M $HClO_4$, 50% AcOH			442[c]	7
(*E*)-3-phenyl-2-propenoate	KH_2PO_4–Na_2HPO_4	6.80	0.80	588	9
	KH_2PO_4–K_2HPO_4	6.50	0.80	490	4
	Na_2SiO_3	11.3		742	8
	0.5 M NaOH			864	8
	0.1 M KOH	13.0		503	4
(*E*)-3-(2-thienyl)-2-propenoate	KH_2PO_4–Na_2HPO_4	6.80	0.80	1333	1
(*E*)-3-(3-thienyl)-2-propenoate	KH_2PO_4–Na_2HPO_4	6.80	0.80	1071	1
(*E*)-3-(2-pyridinyl)-2-propenoate	KH_2PO_4–Na_2HPO_4	6.80	0.80	928[d]	this work
(*E*)-3-(3-pyridinyl)-2-propenoate	KH_2PO_4–Na_2HPO_4	6.80	0.80	687[e]	this work
(*E*)-3-(4-pyridinyl)-2-propenoate	KH_2PO_4–Na_2HPO_4	6.80	0.80	1195	this work

[a] Temperature = 25.0 °C, λ = 526 nm. [b] Ionic strength. [c] Temperature = 30.0 °C. [d] Rate at 418 nm = k = 1187 $M^{-1}\ s^{-1}$. [e] Rate at 418 nm = k = 610 $M^{-1}\ s^{-1}$.

An increase in buffer concentration will result in an increase in the amount of phosphate ions adsorbed on colloidal manganese dioxide, which will lead to a decrease in the rate of flocculation owing to the accumulated negative electrostatic charges on the colloid surfaces. Consequently, at higher buffer concentrations, the smaller sizes of the colloidal particles lead to a decrease in the scattering of light (Rayleigh's law, Figure 2)[1,9,30,31] and good pseudo-first-order rate plots for formation of manganese dioxide. Similar Rayleigh's law plots (Figure 2) were obtained for (*E*)-3-(2-pyridinyl) and (*E*)-2-methyl-3-(3-pyridinyl)-2-propenoate (5 and 9).

Although the composition of the complexed soluble (colloidal) manganese dioxide is not known,[10,12] the ultraviolet–visible spectral data from the oxidation of 6 and 7 are consistent with a manganese(IV) species (Figure 3).[1,3,6,9,10,33–40]

Table III. Substituent Effects on the Permanganate Ion Oxidation of (*E*)-2-Propenoates[a]

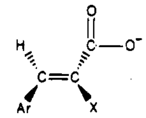

Ar	X	k^b $M^{-1}\ s^{-1}$	k^c relative	ref
6-methyl-2-pyridinyl	H	1039[d]	1.10	this work
4-methylphenyl	H[e]	801	1.30	9
4-methylphenyl	H[f]	407	0.90	7
2-methyl-2-thienyl	H	1473	1.10	1
5-methyl-2-thienyl	H	1436	1.10	1
3-pyridinyl	CH_3	215[g]	0.27	this work
phenyl	CH_3	271	0.40	3
2-thienyl	CH_3	188	0.14	1
3-thienyl	CH_3	287	0.27	1
3-pyridinyl	CN	1281[h]	1.78	this work
phenyl	CN	1134	1.64	3
2-thienyl	CN	133	0.10	1
3-thienyl	CN	514	0.48	1

[a] Temperature = 25.0 °C unless otherwise noted; λ = 526 nm; [KH_2PO_4] = [Na_2HPO_4] = 0.20 M; pH 6.83 ± 0.03; ionic strength (μ = 0.80). [b] Second-order rate constant = k = k_ψ/[substrate]. [c] Rate constant for substituted compound divided by rate constant for unsubstituted compound = k_X/k_H. [d] Rate at 418 nm = k = 1176 $M^{-1}\ s^{-1}$. [e] Ionic strength = 1.60. [f] (*E*)-(4-Methylphenyl)-2-propenoic acid is substrate in 1.01 M $HClO_4$–50% CH_3CO_2H. [g] Rate at 418 nm = k = 227 $M^{-1}\ s^{-1}$. [h] Rate at 418 nm = k = 1287 $M^{-1}\ s^{-1}$.

Although heterogeneous and homogeneous autocatalysis has been detected during the reaction of permanganate ion and various substrates,[26–30,36,41–46] it has been shown[29] that addition of phosphate ions inhibited the catalytic decomposition of permanganate ion by manganese dioxide in acid solution.[46] The linearity of the pseudo-first-order plots at 526 nm and 418 nm suggests an absence of autocatalysis by manganese dioxide.[32,40]

Table II shows that under identical experimental conditions phenyl-, pyridinyl- and thienyl-2-propenoates are oxidized by permanganate ion at similar rates, which may suggest that permanganate ion is neither electrophilic nor nucleophilic. Pyridine, a π-deficient heterocycle, has a —N= in place of —CH= in benzene, the model aromatic compound. The higher electronegativity of nitrogen distorts the π-electron distribution by its inductive ability so that the π-electron density at nitrogen is increased and the electron densities at the carbon sites in the ring are decreased relative to the carbon sites in benzene. Thus, the π-electron density in the double bonds of 3-pyridinyl-2-propenoate is expected to be less than that in 3-phenyl-2-propenoate. In contrast, the strong resonance donor ability of the thiophene ring (π-excessive heterocycle) overides its inductive withdrawal effect. Thus, if permanganate ion is electrophilic, it would be expected to react faster with 3-thienyl-2-propenoate than with 3-

---

(30) (a) Mata, F.; Pérez-Benito, J.; Arranz, A. *Z. Phys. Chem* **1983**, *135*, 141. (b) Mata-Pérez, F.; Pérez-Benito, J. *Z. Phys. Chem.* **1984**, *141*, 213. (b) Mata, F.; Pérez-Benito, J. *An. Quim.* **1985**, *81*, 79.

(31) Mata-Pérez, F.; Pérez-Benito, J. F. *Can. J. Chem.* **1985**, *63*, 988.

(32) In this study, the stabilizing agents are probably HPO_4^{2-} and $H_2PO_4^-$ owing to the low concentration of PO_4^{3-} near neutral pH.

(33) Cooper, S. R.; Calvin, M. *J. Am. Chem. Soc.* **1977**, *99*, 6623.

(34) Magers, K. D.; Smith, C. G.; Sawyer, D. T. *Inorg. Chem.* **1978**, *17*, 515.

(35) Jâky, M.; Simândi, L. I., unpublished results.

(36) Lee, D. G.; Pérez-Benito, J. F. *Can. J. Chem.* **1985**, *63*, 1275.

(37) Perez-Benito, J. F.; Lee, D. G. *Can. J. Chem.* **1985**, *63*, 3545.

(38) (a) Simândi, L. I.; Jâky, M.; Savage, C. R.; Schelly, Z. A. *J. Am. Chem. Soc.* **1985**, *107*, 4220. (b) Simândi, L. I.; Jâky, M.; Schelly, Z. A. *J. Am. Chem. Soc.* **1984**, *106*, 6866.

(39) Jâky, M.; Shafirovich, V. Ya.; Simandi; L. I. *Inorg. Chim. Acta* **1984**, *90*, L39.

(40) The soluble (colloidal) form of manganese(IV) observed in various oxidations by permanganate ion can also be prepared by dissolving freshly precipitated MnO_2 in phosphoric acid.[39] Although the structure of this manganese(IV) species remains to be established, it may have a dinuclear phosphotomanganese(IV) structure.[29,34,35,38]

(41) Morse, H. N.; Hopkins, A. J.; Walker, M. S. *Am. Chem. J.* **1986**, *18*, 401.

(42) Wei, M.-M.; Stewart, R. *J. Am. Chem. Soc.* **1966**, *88*, 1974.

(43) Stewart, R. *Oxidation Mechanisms: Applications to Organic Chemistry*; Benjamin: New York, 1964; p 60.

(44) Fouinat, F.; Magat, M. *J. Chim. Phys.* **1950**, *47*, 514.

(45) Skoog, D. A.; West, D. M. *Fundamentals of Analytical Chemistry*, 2nd ed., Holt, Rinehart, and Winston: Toronto, 1969; p 422.

(46) In contrast, autocatalysis by manganese dioxide has been reported during the permanganate ion oxidation of amines in phosphate-buffered solutions.[30]

Table IV. ^{13}C NMR and ^{1}H NMR Resonances of (*E*)-3-Substituted 2-Propenoic Acids[a]

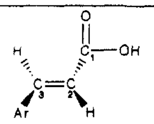		δ_C			δ_H	
	C-1	C-2	C-3	H-2	H-3	$J_{(H\text{-}2\text{-}H\text{-}3)}$, Hz
methyl	172.3	122.5	147.3	5.86	7.07	13.8
phenyl	172.5	117.5	147.3	6.45	6.50	16.0
2-pyridinyl	167.3	124.7	143.2	6.81	7.60	15.8
6-methyl-2-pyridinyl	167.4	124.2	143.3	6.89	6.69	15.7
3-pyridinyl	172.5	117.5	147.3	6.45	6.50	16.0
2-cyano-3-pyridinyl	162.8	106.3	151.8		8.39	
2-methyl-3-pyridinyl	169.0				7.59	
4-pyridinyl[b]				6.32	6.93	16.0
2-thienyl	167.5	117.7	137.1	6.25	7.89	15.6
3-thienyl	168.2	118.8	138.2	6.28	7.75	15.8

[a] $CDCl_3$ solvent. [b] D_2O + KOH solvent.

Table V. Activation Parameters for the Permanganate Ion Oxidation of (*E*)-3-Aryl-Substituted 2-Propenoates[a]

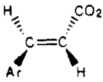 Ar	$\Delta G^{\ddagger}$, kJ mol^{-1}	$\Delta H^{\ddagger}$ kJ mol^{-1}	$\Delta S^{\ddagger}$, J K^{-1} mol^{-1}
phenyl[b]	57.0	14.7	153
2-pyridinyl	58.4	19.6	122
3-pyridinyl	56.7	11.7	151
2-thienyl[c]	55.3	12.7	143

[a] In 0.20 M KH_2PO_4–Na_2HPO_4, μ = 0.80, λ = 525 nm. [b] Reference 9; in 0.05 M KH_2PO_4–Na_2HPO_4. [c] Reference 1.

pyridinyl-2-propenoate (Table II, III).

The oxidation of vinyl ethers by permanganate ion is accelerated by both electron-withdrawing and electron-donating groups,[47,48] and a concave upward Hammett plot has been observed for the permanganate ion oxidation of substituted 1,2-diphenylethenes.[48,49] An ambiphilic permanganate ion is expected to exhibit a parabolic dependence on alkene π-electron availability that is characterized by high reactivity toward both electron-poor and electron-rich alkenes and low reactivity toward alkenes of intermediate electronic character.[47-49]

Chemical shifts of the protons in aromatic molecules reflect the electron density at the carbon atoms to which they are attached. An empirical linear correlation between ^{13}C NMR chemical shifts (δ_C) and the π-electron densities (q) calculated by using a simple Hückel MO treatment has been observed. These examples illustrate the validity of using δ_C to estimate the charge density at carbon.[50] However, a plot of log k vs. the average value of δ_C for the carbon atoms of the double bond in (*E*)-3-aryl-2-propenoates (Table IV) does not show significant substrate dependence on the rate of oxidation.[51]

It must be noted that the ^{13}C NMR chemical shift can at best give a picture of the electron density at carbon in the ground state. A strong mesomeric contribution from the heteroatom in the transition state would influence the rate of oxidation. The sterically undemanding cyano group, being a strong electron-withdrawing substituent, can inductively or by resonance lower the electron density of the carbon–carbon double bond.[52,53] A predominance of one or several of these factors would influence the philicity of permanganate ion.

The activation parameters (Table V) and kinetic data are consistent with highly ordered activated complexes of variable charge development.[47-49] A plot of $\Delta H^{\ddagger}$ vs. $\Delta S^{\ddagger}$ often will be reasonably linear for a series of closely related reactions. A plot of the data in Table V shows that phenyl appears to be quite displaced from a line generated by the three heterocyclic cases. Thus, phenyl may be operating under quite a different mechanism than the other three. Presumably, depending on the demands of the substituents, the oxidation proceeds via an electron-deficient or an electron-rich activated complex that concurrently controls the philicity of permanganate ion.[47-49]

Although the manganese(VII) in permanganate ion is surrounded by oxygens and high electron density, it may form a charge-transfer complex with an alkene that rapidly goes to metallacycle 1.[1,9,13,14,50,55] Rearrangement of metallacycle 1 to the cyclic manganate(V) diester 2 is consistent with the results of this study and other investigations.

Acknowledgment. We thank Professor Lâszlo I. Simândi (Hungarian Academy of Sciences) for valuable discussions and the National Science Foundation for the purchase of the stopped-flow spectrometer (CHE 77-07970) and for financial assistance toward the purchase of the NMR spectrometers.

Registry No. **5**, 54495-51-1; **6**, 19337-97-4; **7**, 84228-93-3; **8**, 106988-32-3; **9**, 106988-33-4; **10**, 106988-34-5.

---

(47) Toyoshima, K.; Okuyama, T.; Fueno, T. *J. Org. Chem.* **1980**, *45*, 1600.

(48) (a) Lee, D. G.; Brown, K. C. *J. Am. Chem. Soc.* **1982**, *104*, 5076. (b) Lee, D. G.; Brown, K. C.; Karaman, H. *Can. J. Chem.* **1986**, *64*, 1054.

(49) Henbest, H. B.; Jackson, W. R.; Robb, B. C. G. *J. Chem. Soc. B.* **1966**, 803.

(50) (a) Olah, G. A.; White, A. M.; O'Brien, D. H. In *Carbonium Ions*; Olah, G. A., Schleyer, P. v. R., Eds.; Wiley-Interscience: 1973; Vol. 4, p 1697. (b) Young, R. N. *Progress in NMR Spectroscopy*; Pergamon Press: Oxford, 1979; Vol. 12, p 1697. (c) Spiesecke, H.; Schneider, W. G. *Tetrahedron Lett.* **1961**, 468. (d) Fliszar, S.; Cardinal, G.; Beraldin, M.-T. *J. Am. Chem. Soc.* **1982**, *104*, 5287. (e) Strub, H.; Beeler, A. J.; Grant, D. M.; Michl, J.; Cutts, P. W.; Zilm, K. W. *J. Am. Chem. Soc.* **1983**, *105*, 3333. (f) Brown, H. C.; Ramachandran, P. J.; Prasad, J. V. N. *J. Org. Chem.* **1985**, *50*, 5583.

(51) Other studies have also shown that sometimes the permanganate ion oxidation of carbon–carbon double bonds is not very sensitive to substituent effects.

(52) (a) Gassman, P. G.; Saito, K.; Talley, J. J. *J. Am. Chem. Soc.* **1980**, *102*, 7613. (b) Gassman, P. G.; Talley, J. J. *J. Am. Chem. Soc.* **1980**, *102*, 1214, 4138. (c) Krishnamurthy, V. V.; Prakash, G. K. S.; Iyer, P. S.; Olah, G. A. *J. Am. Chem. Soc.* **1986**, *108*, 1575.

(53) (a) Product studies suggest that electron-withdrawing groups on the olefin facilitates its oxidation since fluroalkenes undergo rapid degradation and cleavage.[10,53b,c] (b) Suzuki, H. *Bull. Chem. Soc. Jpn.* **1960**, *33*, 406. (c) Burdon, J.; Tatlow, J. C. *J. Appl. Chem.* (*London*) **1058**, *8*, 293. (d) Oxidation of a cyanoalkene in the steroid series gives a ketol: Tull, R.; Jones, R. E.; Robinson, S. A.; Tishler, M. *J. Am. Chem. Soc.* **1955**, *77*, 196.

(54) Simândi, L. I.; Jâky, M. *J. Chem. Soc., Perkin Trans. 2* **1973**, 1856.

(55) Eisenstein, O.; Hoffman, R. *J. Am. Chem. Soc.* **1981**, *103*, 4308.